Molecular Crystals and Liquid Crystals

ISSN: 1542-1406 (Print) 1563-5287 (Online) Journal homepage: https://www.tandfonline.com/loi/gmcl20

Raman spectroscopy of nanoscale carbons and of an isolated carbon nanotube

M. S. Dresselhaus , A. Jorio , G. Dresselhaus , R. Saito , A. G. Souza Filho & M. A. Pimenta

To cite this article: M. S. Dresselhaus , A. Jorio , G. Dresselhaus , R. Saito , A. G. Souza Filho & M. A. Pimenta (2002) Raman spectroscopy of nanoscale carbons and of an isolated carbon nanotube, Molecular Crystals and Liquid Crystals, 387:1, 21-29, DOI: 10.1080/10587250215231

To link to this article: https://doi.org/10.1080/10587250215231

Published online: 18 Oct 2010.

Mol. Cryst. Liq. Cryst., Vol. 387, pp. [245]/21–[253]/29

1058-725X/02 $12.00 + .00
DOI: 10.1080/10587250290113529

RAMAN SPECTROSCOPY OF NANOSCALE CARBONS AND OF AN ISOLATED CARBON NANOTUBE

M. S. Dresselhaus
Dept. of Electrical Engineering and Computer Science, and Dept. of Physics, Massachusetts Institute of Technology, Cambridge, MA 02139-4307, USA

A. Jorio
Dept. of Physics, Massachusetts Institute of Technology, Cambridge, MA 02139-4307, USA

G. Dresselhaus
Francis Bitter Magnet Laboratory, Massachusetts Institute of Technology, Cambridge, MA 02139-4307, USA

R. Saito
Department of Electronic Engineering, University of Electro-Communications, Chofu, 182-8585 Tokyo, Japan

A. G. Souza Filho
Dept. of Physics, Massachusetts Institute of Technology, Cambridge, MA 02139-4307, USA; and Dept. de Física, Univ. Federal do Ceará, Fortaleza-CE, 60455-760 Brazil

M. A. Pimenta
Dept. de Física, Univ. Federal de Minas Gerais, Belo Horizonte-MG, 30123-970 Brazil

The use of Raman spectroscopy as a characterization tool for carbon materials is briefly reviewed with particular emphasis given to nano-carbons and carbon

The authors thank many colleagues for their contributions to this research. R.S. acknowledges a Grant-in-Aid (No. 13440091) from the Ministry of Education, Japan. A.J. and M.A.P./A.G.S.F. acknowledge support from the Brazilian agencies CNP_q/CAPES. The MIT authors acknowledge support under NSF Grants DMR 01-16042, INT 98-15744, and INT 00-00408.

nanotubes. The observation of Raman spectra from one carbon nanotube is discussed, including the new physical phenomena that occur at the single nanotube level, with special emphasis given to the use of resonance Raman scattering for the structural determination of (n, m) for individual nanotubes. Examples are given to show how single nanotube spectroscopy provides insight into the use of Raman spectroscopy for characterizing nanotube bundles and for carrying out other properties measurements on individual carbon nanotubes.

Keywords: carbon nanotubes; Raman spectroscopy; nanotube structural characterization; single nanotube spectroscopy

INTRODUCTION

Single wall carbon nanotubes (SWNTs) are important for the development of the nanoscience field because of the new nanoscience concepts that they introduce. SWNTs furthermore provide a system that is simple enough, so that detailed calculations of their properties can be carried out, and predictions about their behavior can be made. Because of their unique physical properties, carbon nanotubes show great promise also for practical applications.

As summarized here, Raman spectroscopy provides an important characterization tool for carbon-based materials, showing distinctly different characteristic spectra for sp^3, sp^2, sp carbons, disordered carbons, fullerenes and nanotubes. This paper, however, focuses on the use of Raman spectroscopy for the characterization of carbon nanotubes, showing how this technique provides unique information, often not available by other techniques.

Figure 1 demonstrates the distinctive Raman spectra provided by each type of carbon material, from 1D carbynes to 2D graphite to 3D diamond. The different bonding strengths and their implied force constants further differentiates bulk carbons from the nanotube and fullerene carbon nanostructures which are also all different from one another. In addition, Raman spectroscopy has been a key tool for the description and characterization of disorder in the sp^2 bonding in terms of the disorder-induced D-band and D^*-based features shown in Figure 1 at $1350\,\mathrm{cm}^{-1}$ and $1620\,\mathrm{cm}^{-1}$, respectively. It is therefore not surprising to expect that Raman spectroscopy would provide a key tool for the characterization of carbon nanotubes.

Each single wall carbon nanotube (SWNT) is characterized by two integers (n, m). These integers specify the number of unit vectors $\vec{a}_1$ and $\vec{a}_2$ in the graphene honeycomb structure that constitute the chiral vector (or roll-up vector) $\vec{C}_h = n\vec{a}_1 + m\vec{a}_2$ corresponding to the nanotube circumference. These (n, m) indices also determine the nanotube diameter

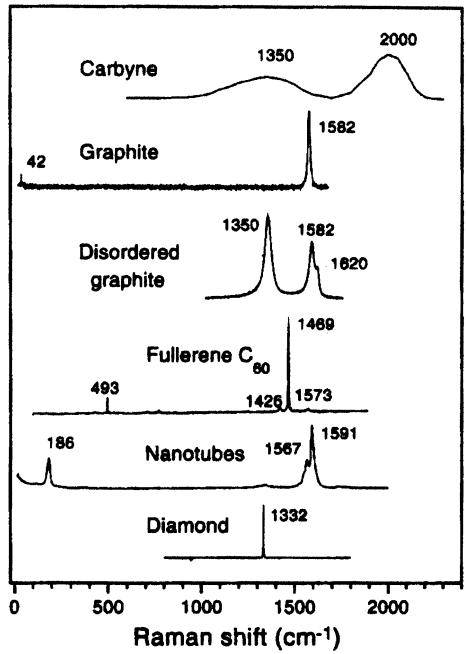

FIGURE 1 (a) Raman spectra from various carbon-based materials: carbyne (sp bonded carbon), graphite (sp^2 bonded carbon), fullerene C_{60}, carbon nanotubes, and diamond (sp^3 bonded carbon).

and chirality, or the orientation of the carbon hexagons with respect to the nanotube axia. Raman spectra of the radial breathing mode, whereby every carbon atom in the nanotube vibrates in phase in the radial direction, give a direct measure of the nanotube diameter, because the radial breathing mode frequency ω_{RBM}, is proportional to the inverse diameter of the nanotube. The electronic properties of SWNTs are remarkable insofar as they can be either metallic (when $m-n=3q$ and q is an integer) or semiconducting (when $n - m = 3q \pm 1$). Raman spectroscopy can be used to distinguish between metallic and semiconducting tubes, because of their very different spectral lineshapes.

The large density of electronic states for one-dimensional (1D) systems and the strong electron-phonon coupling under resonance conditions allow observation of the Raman spectra from one individual single wall carbon nanotube (see Fig. 2), when the incident or scattered photon is in resonance with an interband transition between 1D singularities in the joint density of states (JDOS) between the valence and conduction bands. The enhancement of the signal coming from the resonance with these

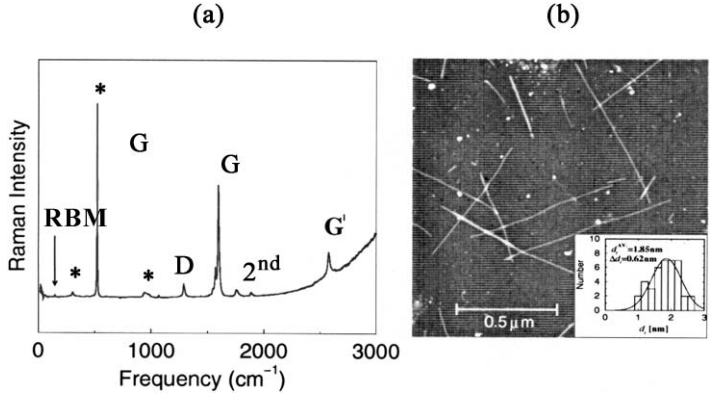

FIGURE 2 (a) Raman spectrum from one nanotube taken over a broad frequency range using $E_{\text{laser}} = 785\,\text{nm} = 1.58\,\text{eV}$ excitation, and showing the radial breathing mode (RBM), the D-band, the G-band, second-order features, and the G′-band. The features marked with '*' at 303 cm^{-1}, 521 cm^{-1} and 963 cm^{-1} [1] are from the Si/SiO_2 substrate and are used for calibration of the nanotube Raman spectrum. (b) AFM image of the sample showing isolated single wall nanotubes grown from the vapor phase [2]. The small particles are iron catalyst particles. The inset shows the diameter distribution of this sample based on AFM observations of 40 SWNTs [3].

singularities in the JDOS can be very large, so that in some cases the Raman intensity from one nanotube can be as large as that for the silicon substrate even though the Si/C atom ratio is about 10^6 in the laser excitation beam of 1 μm diameter. Such large enhancement factors arise from the highly 1D nature of carbon nanotubes with diameters less that $\sim$2 nm. Furthermore, Raman spectroscopy is not normally a tool for structural characterization, but for the case of 1D carbon nanotubes, the observation of the Raman spectra from an individual nanotube is used to provide a definitive identification of the nanotube structure through determination of its (n, m) indices. The physical principle that is employed in the (n, m) determination is the trigonal warping effect which causes each (n, m) nanotube to have a unique set of singularities at energies E_{ii} in the JDOS. Resonance Raman scattering allows determination of these energies E_{ii} and the corresponding wave vectors k_{ii} where these singularities occur, thereby providing a determination of the (n, m) indices of the nanotube in resonance with E_{laser}, the laser excitation energy. This information is further used to determine, to high resolution, the profile of the joint density of states near one of its characteristic 1D singularities, showing that the width of the 1D singularities in the density of states is less than 1 meV, thereby explaining how it is possible to get a sharp Raman signal from such a small

nanostructure. Because of the high sensitivity of the electronic, transport, vibrational and other nanotube properties to the structural (n, m) indices, this non-destructive, readily available resonance Raman characterization technique is expected to have a significant impact on current basic research on carbon nanotubes generally, because now it will be possible to study many properties at the single nanotube level as a function of diameter and chirality by combining Raman and other measurement techniques. A few examples of the richness of this newly emerging field of single nanotube spectroscopy are presented here.

Figure 2 shows that each feature in the Raman spectra of single wall carbon nanotubes can now be investigated at the single nanotube level. These features include the non-dispersive radial breathing mode which is not present in other sp^2 carbons and the G-band feature, which is also present in sp^2 carbons but has many distinct properties for nanotubes relative to other sp^2 carbons. Also included in the Raman spectra are the highly dispersive disorder-induced D-band and its second harmonic G′-band, where the mode frequencies show a strong dependence on the laser excitation energy. Such investigations reveal many interesting details about the dependence of each feature in the resonance Raman spectra on nanotube diameter, chirality, metallic vs. semiconducting behavior, but provide in addition an astonishingly sensitive probe of the unique electronic structure of carbon nanotubes. Furthermore, study of the Raman spectra at the single nanotube level allows investigation of new physical phenomena, particularly phenomena about the resonance Raman effect that have never been observed before in any physical system.

Figure 3 gives three examples of what single nanotube spectroscopy tells us about SWNT bundles. Measurements of the radial breathing mode at the single nanotube level yield a relatively narrow Lorentzian line [see Fig. 3(a)] and a determination of the nanotube diameter by the relation $d_t = 248/\omega_{\mathrm{RBM}}$. The spectrum for the bundle shows a superposition of Raman signal from all tubes resonant with $E_{\mathrm{laser}} = 1.58\,\mathrm{eV}$. The SWNT diameter distribution for a bundle can be obtained indirectly from a detailed analysis of the Raman spectra using resonance Raman theory [5], though the detailed analysis of the spectral properties are best studied at the single nanotube level.

As another example of what can be learned by single nanotube spectroscopy, consider the dependence of the G-band frequency on nanotube diameter d_t in Figure 3(b), where it is seen that ω_G^+ for vibrations along the nanotube axis is independent of d_t for both semiconducting and metallic SWNTs, but the vibrations in the circumferential direction ω_G^- show a $\mathcal{C}/d_t^2$ dependence, where the value of $\mathcal{C}$ is nearly twice as large ($\mathcal{C}_M = 79.5\,\mathrm{cm^{-1}\,nm^2}$) for metallic SWNTs as for semiconducting SWNTs ($\mathcal{C}_S = 47.7\,\mathrm{cm^{-1}\,nm^2}$). Furthermore, no chirality dependence is observed for

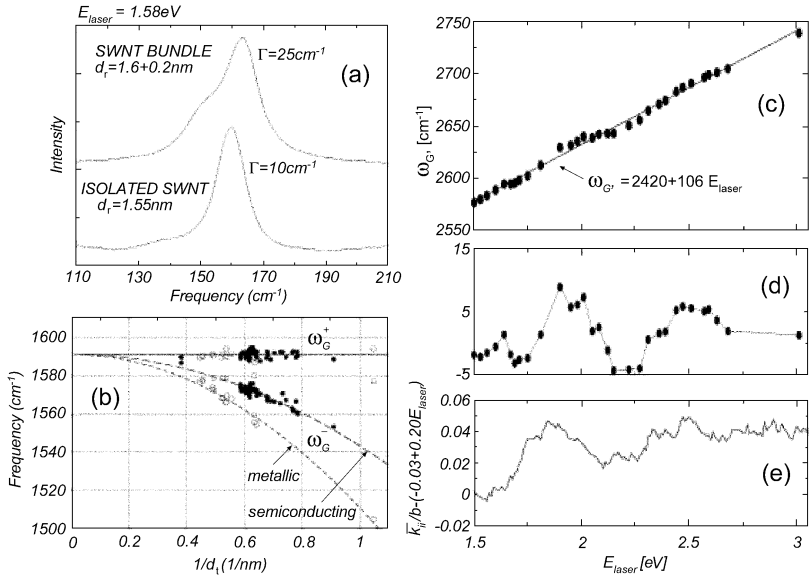

FIGURE 3 (a) RBM Raman spectra for one isolated nanotube and for carbon nanotube bundles. (b) G-band splitting showing diameter dependence of the circumferential and axial modes. (c) G′-band data for ω'_G for a SWNT bundle sample taken from Ref. [4]. (d) Same $\omega_{G'}$ data after subtracting the linear dispersion $2420 + 106E_{\text{laser}}$. (e) Calculated first moment $\bar{k}_{ii}$ for the possible resonant tubes as a function of E_{laser} after subtracting the linear dispersion $-0.03 + 0.20E_{\text{laser}}$.

$\omega_G^{\pm}$, indicating that nanotube curvature is more important than chirality for interpreting the nearest neighbor in-plane carbon-carbon vibrations that stem from the basic vibrations observed in all sp^2 carbons, in support of one model calculation for the G-band phonon eigenvectors [6] and in conflict with another [7]. One use of Figure 3(b) for the analysis of Raman spectra from SWNT bundles is the estimation of the mean diameters for semiconducting and metallic nanotubes contained in the bundle, which can be used as an internal check on the diameter determination based on the radial breathing mode. Another application of Figure 3(b) is for estimating d_t for SWNTs that are in resonance with the scattered photon, so that the radial breathing mode would not in this case be in resonance with E_{laser}, and consequently (n, m) cannot then be determined from the RBM spectrum.

The origin of the disorder-induced Raman peak (D-band), which is observed around $1350\,\text{cm}^{-1}$ for laser excitation energy $E_{\text{laser}} = 2.41\,\text{eV}$ [3,4] in both graphite and single wall carbon nanotubes [11–13], has been explained by a double resonance Raman process involving a second-order scattering process and a Raman intensity enhancement due to the

resonance with both an intermediate state, and also resonance with either the initial or final states thus yielding a double resonance process [13,14].

The third example in Figure 3(c) shows very large dispersion of the G'-band frequency $\omega_{G'}$ as a function of E_{laser} for a SWNT bundle [4]. After subtracting the strong linear term in $\omega_{G'}(E_{\text{laser}})$ that is also observed at approximately the same large magnitude for other sp^2 carbons, an oscillatory component unique to the $\omega_{G'}(E_{\text{laser}})$ dispersion for SWNTs remains, as shown in Figure 3(d). The physical basis of these oscillations stems from the mechanism responsible for the special role of the singularities of the 1D JDOS in the double resonance mechanism for the G' band of sp^2 carbons [5]. In the basic second-order scattering process for the G'-band in sp^2 carbons, an electron with momentum k is (a) excited, (b) scattered to $k + q$ states and (c) back-scattered to the k states, and finally (d) recombining with holes to emit a photon. If two of three intermediate states correspond to real electronic states in the energy dispersion $E(k)$, the Raman intensity is enhanced by two factors in the denominator of the intensity formula, thereby constituting the double Resonance Raman process. For the G'-band second-order process, two phonons of wave vectors q and $-q$ are emitted in the second-order scattering processes.

The dispersion of the G'-band is very important for providing information about electronic processes in carbon nanotubes. In addition to the double resonance process for sp^2 carbons, the energies of the singularities in the 1D electronic JDOS govern the choice of nanotubes that are in resonance with E_{laser}, namely SWNTs that have E_{ii} singularities close in energy to E_{laser}. The k_{ii} wave vector corresponding to each E_{ii} value will strongly couple to a phonon with wave vector $q \simeq 2k_{ii}$. Each E_{ii} band for metallic or semiconducting SWNTs gives rise to an oscillatory behavior in Figure 3(d), with the oscillation centered at 1.9 eV associated with E_{11}^M interband transitions and the oscillation centered at 2.5 eV associated with E_{33}^S and E_{44}^S which lie too close together to be separated from one another. For each SWNT, resonance is possible with either the incident photon, the scattered photon or with the intermediate state $k_{ii} + q$ resulting from the phonon scattering event in the double scattering process. By considering all possible SWNTs in the SWNT bundle that can contribute to each of the E_{11}^M, E_{33}^S and E_{44}^S-bands, the curve shown in Figure 3(e), is obtained. The detailed behavior that is observed in Figures 3(d) for the phonons and 3(e) for the electron k_{ii} vectors arises from the detailed dependence of the k_{ii} values on nanotube diameter ($\omega_{G'}$ decreases as d_t decreases) and on the chiral angle which has been calculated [5].

The large dispersion of the G' band allows observation of new physical phenomena, not seen in other systems. For example, for the case of semiconducting nanotubes, it is possible at the single nanotube level for the incident photon to be resonant with the E_{44}^S level of that SWNT and the

scattered photon to be resonant with E_{33}^{S} for a very special subset of SWNTs that can be predicted theoretically. This special subset is strongly dependent on the (n, m) assignment [3] and shows two peaks in the G'-band spectra for the two resonant processes. The excellent agreement between experiment and theory on which tubes show this two peak effect gives strong confirmation for the method used to obtain the (n, m) assignments from the analysis of the radial breathing mode feature.

For metallic SWNTs at the single nanotube level, the splitting of the singularities in the electronic JDOS due to the trigonal warping effect [16] can be measured quantitatively by measuring the shift $\Delta\omega_{G'}$ in the G'-band structure associated with each van Hove singularity involved in the splitting of the electronic states ΔE_{ii}^{M} for metallic nanotubes due to trigonal warping. The splitting ΔE_{ii}^{M} is zero for armchair SWNTs and a maximum for zigzag SWNTs. Since each component of ΔE_{ii}^{M} has different electronic energies in the trigonally split singularities in the JDOS, each of the components will have different k_{ii}-vectors, thereby giving rise to different q values for the G' band phonons and finally different $\omega_{G'}$ values will be obtained with a peak separation of $\Delta\omega_{G'}$. By measuring these splittings $\Delta\omega_{G'}$ in the ω'_G profiles for SWNTs with different chirality, it is possible to determine the dependence of $\Delta\omega_{G'}$ on ΔE_{ii}^{M}. The linear relation observed experimentally for $\Delta\omega_{G'}$ vs. ΔE_{ii}^{M} for different isolated SWNTs gives an independent determination of $108 \pm 5\,\mathrm{cm}^{-1}/\mathrm{eV}$ for the dispersion of $\omega_{G'}$ as a function of E_{laser}, even though the measurements are all made using one laser line [16]! The excellent agreement of this value with $\partial\omega_{G'}/\partial E_{\mathrm{laser}} = 106\,\mathrm{cm}^{-1}/\mathrm{eV}$ obtained from measurements on SWNT bundles using many laser lines [4] is important in understanding the relation between single nanotube spectroscopy and the G'-band spectra obtained from bundles. The consistency of these two determinations of the dispersion of $\omega_{G'}$ vs. E_{laser} gives further support for the method used for the (n, m) determination.

In conclusion, single nanotube spectroscopy opens up many new possibilities for carbon nanotube research, leading to the discovery of many new physical phenomena, and a better understanding of what is actually observed in the Raman spectroscopy of nanotube bundles. Single nanotube spectroscopy also provides a basis for using Raman characterization to carry out quantitative studies of other physical phenomena (e.g., transport, mechanical properties) at the single nanotube level.

REFERENCES

[1] Temple, P. A. & Hathaway, C. E. (1973). *Phys. Rev. B*, *7*, 3685–3697.
[2] Hafner, J. H., Cheung, C. L., Oosterkamp, T. H., & Lieber, C. M. (2001). *J. Phys. Chem. B*, *105*, 743.

[3] Jorio, A., Saito, R., Hafner, J. H., Lieber, C. M., Hunter, M., McClure, T., Dresselhaus, G., & Dresselhaus, M. S. (2001). *Phys. Rev. Lett.*, *86*, 1118–1121.
[4] Pimenta, M. A., Hanlon, E. B., Marucci, A., Corio, P., Brown, S. D. M., Empedocles, S. A., Bawendi, M. G., Dresselhaus, G., & Dresselhaus, M. S. (2000). *Brazilian J. Phys.*, *30*, 423–427.
[5] Milnera, M., Kurti, J., Hulman, M., & Kuzmany, H. (2000). *Phys. Rev. Lett.*, *84*, 1324–1327.
[6] Saito, R., Dresselhaus, G., & Dresselhaus, M. S. (1998). *Physical Properties of Carbon Nanotubes* (Imperial College Press, London).
[7] Reich, S., Thomsen, C., Duesberg, G. S., & Roth, S. (2001). *Phys. Rev. B*, *63*, 1401R.
[8] Tuinstra, F. & Koenig, J. L. (1970). *J. Chem. Phys.*, *53*, 1126.
[9] Dresselhaus, M. S. & Eklund, P. C. (2000). *Advances in Physics*, *49*, 705–814.
[10] Dresselhaus, M. S., Dresselhaus, G., Jorio, A., Souza Filho, A. G., & Saito, R. (2002). *Carbon*, *40*, 2043 10/13/01: LRR-66/01.
[11] Saito, R., Jorio, A., Souza Filho, A. G., Dresselhaus, G., Dresselhaus, M. S., & Pimenta, M. A. (2002). *Phys. Rev. Lett.*, *88*, 27401.
[12] Kürti, J., Zólyomi, V., Grüeneis, A., & Kuzmany, H. (2001). *Phys. Rev. B*, submitted.
[13] Thomsen, C. & Reich, S. *Phys. Rev. B*, *65*, 165433.
[14] Martin, R. M. & Falicov, L. M. (1975). In *Light Scattering in Solids: edited by M. Cardona*, page 80, (Springer-Verlag, Berlin).
[15] Souza Filho, A. G., Jorio, A., Dresselhaus, G., Dresselhaus, M. S., Saito, R., Swan, A. K., Ünlü, M. S., Goldberg, B. B., Hafner, J. H., Lieber, C. M., & Pimenta, M. A. (2002). *Phys. Rev. B*, *64*, submitted: 8/28/01:MS BH8324: accepted 9/26/01: AIP 077147PRB.
[16] Souza Filho, A. G., Jorio, A., Samsonidze, Ge. G., Dressehaus, G., Dresselhaus, M. S., Swan, A. K., Ünlü, M. S., Goldberg, B. B., Saito, R., Hafner, J. H., Lieber, C. M., & Pimenta, M. A. (2002). *Chem. Phys. Lett.*, *354*, 62.